Chlorophyll bloom in the western Pacific at the end of the 1997–1998 El Niño: The role of the Kiribati Islands

M. Messié,[1] M.-H. Radenac,[1] J. Lefèvre,[2] and P. Marchesiello[3]

Received 13 February 2006; revised 17 May 2006; accepted 26 May 2006; published 18 July 2006.

[1] During the transition between El Niño and La Niña conditions in 1998, a dramatic bloom occurred near the equator around 170°E, with chlorophyll concentrations reaching more than 0.8 mg m^{-3} in May. Previous studies attributed this bloom to a wind-driven upwelling and to the shoaling of the Equatorial Undercurrent (EUC), but they did not explain its particular location near the Kiribati Islands. By combining simulations with observations, we determined that these islands were able to locally disrupt the physical dynamics and the nutrient fields to the extent that they were directly responsible for the location and the amazing strength of the bloom. Our results suggest that an island mass effect was responsible for generating the bloom, while the barrier formed by the islands increased EUC shoaling to the west of them, which explained the bloom peak. **Citation:** Messié, M., M.-H. Radenac, J. Lefèvre, and P. Marchesiello (2006), Chlorophyll bloom in the western Pacific at the end of the 1997–1998 El Niño: The role of the Kiribati Islands, *Geophys. Res. Lett.*, *33*, L14601, doi:10.1029/2006GL026033.

1. Introduction

[2] The 1997–98 El Niño was the strongest event of the century, both in terms of physical and biological records. It also coincided with the launching of the Sea-viewing Wide Field-of-view Sensor (SeaWiFS) in September 1997, which for the first time, enabled large scale studies of the biological consequences of El Niño to be undertaken. In particular, at the end of this event, dramatic increases in chlorophyll concentration occurred in different areas of the equatorial Pacific basin [*Ryan et al.*, 2002]. This paper focusses on a bloom which took place along the equator near 170°E (Figure 1a), during the transition between El Niño and La Niña (March–June 1998). This bloom was exceptional in size (almost 500,000 km^2), in length, and in strength, with chlorophyll concentrations reaching more than 0.8 mg m^{-3} in May, in a region where the average concentration (1998–2004) hardly reaches 0.15 mg m^{-3}.

[3] Several authors have explained the bloom by means of different mechanisms. *Murtugudde et al.* [1999] observed a reduction in barrier layer thickness in model simulations, and attributed the bloom to a wind-driven upwelling and to turbulent vertical mixing. *Wilson and Adamec* [2001] pointed out that it coincided with the reappearance and shoaling of the Equatorial Undercurrent (EUC), which is said to be the major source of iron for the High Nutrient Low Chlorophyll (HNLC) equatorial ecosystem [*Gordon et al.*, 1997]. A synthesis, conducted by *Ryan et al.* [2002], concluded that the bloom resulted from both wind-driven upwelling and vertical mixing, which were efficient because of the anomalously shallow thermocline and EUC following the El Niño event.

[4] However, one point remains unclear: why did the bloom take place in this particular region? In fact, the nutricline and EUC shoaled across the whole equatorial basin [*Radenac et al.*, 2001; *Wilson and Adamec*, 2001]. A careful examination of the SeaWiFS images shows that high-chlorophyll waters appear to originate from islands east of the bloom (Figure 1a). The Gilbert Islands which are part of the Republic of Kiribati, are small coral atolls which rise from the 4000 m deep surrounding abyssal plain. This paper thus describes how a modeling approach coupled with data analysis was undertaken to assess whether the islands contributed in any way to the bloom generation and development. We will show the extent to which the islands disrupted the large-scale circulation, in a way which favored bloom conditions.

2. Data and Model

2.1. Data

[5] In-situ and satellite data were used to assess the physical and biological context of the bloom and to validate the model outputs (1997–1998). Surface chlorophyll concentrations were SeaWiFS version 4, 9km, 8-day composites obtained from the Distributed Active Archive Center at NASA Goddard Space Flight Center. Sea Surface Temperatures (SST) were taken from Tropical Rainfall Measuring Mission (TRMM) Microwave Imager (TMI) data, produced by Remote Sensing Systems (1/4° × 1/4° weekly maps). Sea level anomalies (SLA) were a TOPEX/Poseidon-ERS2 combined product delivered by the Space Oceanography Division of CLS (1/3° × 1/3° weekly maps). We also used 5-day temperature profiles recorded at the 165°E and 180° moorings (Figure 1, white stars), and ADCP zonal current profiles recorded at the 165°E equatorial mooring from the Tropical Atmosphere Ocean/Triangle Trans-Ocean buoy Network (TAO/TRITON).

2.2. Numerical Model

[6] The Regional Ocean Modeling System (ROMS) is a split-explicit, free-surface, topography-following-coordinate ocean model [*Shchepetkin and McWilliams*, 2005]. The grid is set to 160°E–178°W, 6°S–11°N, with a resolution of 1/6°, and 30 vertical levels with surface refinement are taken into account. The model is forced along its boundaries with 5-day outputs of a 2° global configuration of the Ocean

[1]Laboratoire d'études en géophysique et océanographie spatiales, CNRS, IRD, UPS, CNES, Toulouse, France.
[2]Centre IRD de Nouméa, Nouméa, New Caledonia.
[3]Centre IRD de Bretagne, Plouzané, France.

0094-8276/06/2006GL026033

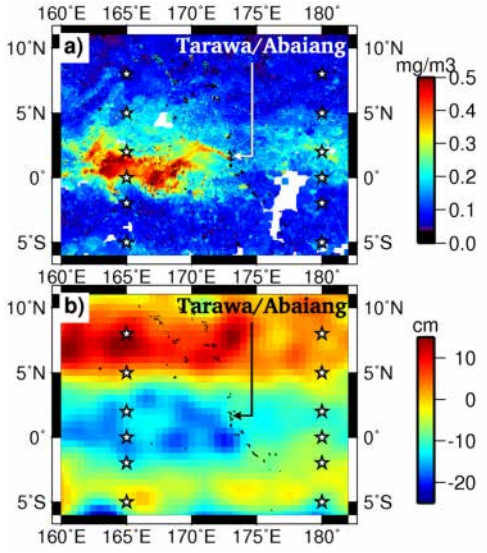

Figure 1. ROMS domain: (a) SeaWiFS chlorophyll (mg m^{-3}, white areas: clouds), 22–28 March and (b) TOPEX/Poseidon – ERS SLA (cm), 29 March – 4 April (1998). White stars indicate TAO buoys.

Parallel (OPA) model (S. Cravatte et al., Progress in the 3-D circulation of the eastern Equatorial Pacific in a climate ocean model, submitted to *Ocean Modelling*, 2006). Wind forcing is calculated from daily wind stress derived by combining TAO data with ERS scatterometer data, and other atmospheric forcing is computed from NCEP 6-hour reanalysis. We ran the model for the 1996–1998 period with two different grids: first, the bathymetry included the Kiribati Archipelago (run K), second, the depth of the abyssal plain (4000 m) was ascribed to the islands location (run NK).

[7] Satellite SST and SLA were in very good agreement with run K outputs, although a cold bias (1998 average: 0.4°C) was found in the bloom region. The average and standard deviation of simulated vertical profiles of temperature were consistent with TAO data at all locations. The vertical structure of zonal currents was well simulated, however, the EUC was slower in the model (especially from June 1998 onward) and its shoaling was weaker than in the TAO data (Figure 2a).

3. Satellite and in Situ Bloom Study

3.1. Bloom Generation: An Island Mass Effect?

[8] In January 1998, primary production was nitrate-limited with chlorophyll concentrations typical of the warm pool oligotrophic ecosystem in which the thermocline matches the nutricline [*Chavez et al.*, 1999]. At the same time, the EUC was either very weak or absent and the nutricline was unusually shallow across the equatorial Pacific. Both chlorophyll and SLA data clearly showed a sharp step near the islands (Figures 3a and 3b). This suggests an island mass effect, defined as an increase of chlorophyll concentration and biological productivity downstream of an oceanic island. The 170°E bloom was downstream when the westward South Equatorial Current (SEC) was flowing, from January to April as seen from TAO data at 165°E (Figure 2a), during the bloom generation. The major enrichments occurred west of the Tarawa/Abaiang group of islands (1.5°N) in SeaWiFS data (Figure 1a).

[9] Since the Kiribati Islands are low coral atolls, land erosion is unlikely to shed nutrients into surface waters. Consequently, possible mechanisms would be upwelling and thermocline uplift in the lee of the islands, and mixing in eddies formed by the flow disturbance, which is coherent with the observed cold satellite SST (not shown) and low SLA data downstream of the islands (Figures 1b and 3b). The characteristics of the wake past an isolated low-latitude island [*Heywood et al.*, 1996] can be predicted from the Reynolds number (Re = UL/ν), where ν is the horizontal eddy viscosity (100 m^2 s^{-1}), L the dimension of the island (80 km for Tarawa/Abaiang), and U the incident current speed (0.5 m s^{-1} from run K outputs and TAO data). We obtained Re = 400, which should be compared with the threshold for eddy shedding: 70 [*Heywood et al.*, 1996]. This meant that a Von Karman vortex street was expected, and strong mixing within eddies would enhance the effect of upwelling-favorable winds. The subsequent nutrient input from a deeper layer could explain the bloom generation. However, compared to the study of *Heywood et al.* [1996], the island is part of an archipelago, thus, this simple scale study only gives a hint of such turbulent processes.

3.2. Bloom Peak: A Sudden Input of Iron?

[10] Chlorophyll concentrations west of the islands increased slowly during the bloom generation. In February, they reached values similar to the ones usually measured in the HNLC ecosystem of the central Pacific. Around mid-April, they abruptly increased, reaching 0.7 mg m^{-3} on a 0°N–2°N average in less than two weeks (Figure 3a). The EUC reappeared in January, gradually strengthened and shoaled, and induced a reversal of zonal currents in the euphotic zone (about 50 m; *Ryan et al.* [2002]) in April–May (Figure 2a). Thus an island wake effect cannot explain the highest chlorophyll concentrations observed at the same time on the west side of the islands. Since the peak of the bloom coincided with the iron-rich EUC shoaling into the euphotic zone, we suggest, following *Wilson and Adamec*

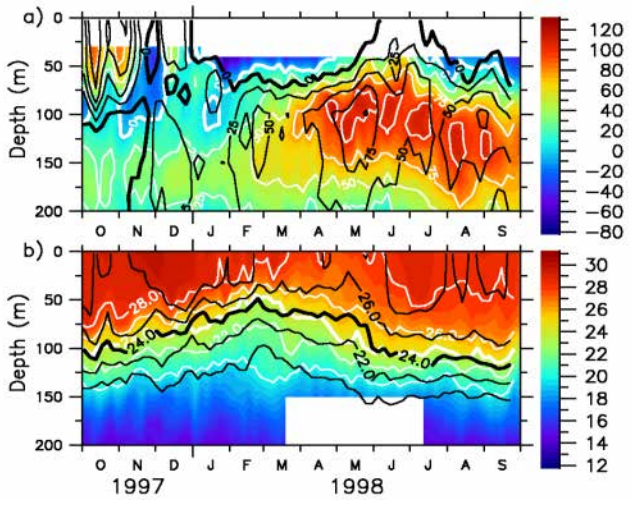

Figure 2. At 165°E, 0°N: (a) zonal currents (cm s^{-1}) and (b) temperature profiles (°C) from TAO data (color and white lines) and run K outputs (black lines).

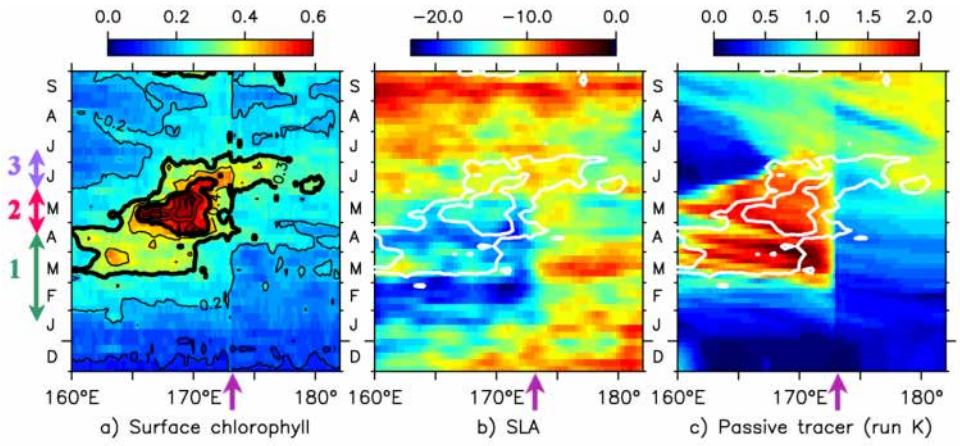

Figure 3. 0°N–2°N longitude-time plots of (a) SeaWiFS chlorophyll concentration (mg m^{-3}); (b) TOPEX/POSEIDON SLA (cm); and (c) run K passive tracer concentration (dimensionless). The bloom domain is overlaid on Figures 3b and 3c as a white line. The purple arrows indicate the islands position. Colored arrows show the three phases of the bloom: 1- bloom generation (green), 2- bloom peak (red), 3- bloom demise (blue).

[2001], that the dramatic increase of chlorophyll concentrations was due to a sudden input of iron. The bloom intensity then dropped as it was advected eastward past the islands, probably because of EUC surfacing. By the end of June, chlorophyll concentrations and SST were back to climatological levels.

4. Numerical Experiments

[11] In order to assess the role of the Kiribati Islands in the regional dynamics, to verify the occurrence of an island mass effect during the growth of the bloom as expected from the theory and to test the hypothesis of a sudden input of iron in mid-April, we compared run K (with Kiribati Islands) and run NK (no islands) outputs.

4.1. Role of Kiribati Islands in the Regional Dynamics

[12] Flow disturbance by the Kiribati Islands clearly affected run K outputs. We observed meanders and eddies appearing downstream of the islands in February, especially behind the Tarawa and Abaiang atolls and these developed as the incident current strengthened. Simultaneously, cold SST appeared just downstream of the islands, as well as low SLA and high surface water density. Temperature and density isolines rose by 40 m just west of the islands and slightly deepened east of them (Figure 4a) especially from mid-February to May. The EUC shoaled west of the islands, and deepened by more than 40 m east of them (Figure 4b). Meandering, eddy formation, and isopycnal rise are characteristic of an island mass effect.

4.2. Nitrate Behavior From a Passive Tracer

[13] A passive tracer was used to mimic the behavior of nitrate-rich water masses. Although it follows the advection-diffusion equation, such a tracer is not representative of a modeled nitrate compartment as no sources and sinks are applied. Passive tracer concentrations ([*PasTr*]) were initialized in September 1997 from a nitrate-temperature relationship calculated from the *World Ocean Atlas 2001* data set [*Conkright et al.*, 2002; *Stephens et al.*, 2002]: [*PasTr*] = 0 for T > 24°C, and [*PasTr*] = 27 − 1.1235 × T otherwise. The same conditions were then applied as boundary forcing. The tracer-dyed water mass was advected and mixed in run K, and high surface concentrations, confined west of the islands, were found from March to June (Figure 3c). In run NK (not shown), tracer concentrations notably began to increase only in mid-April, mainly in the eastern part of the domain. High [*PasTr*] (>1.5) in run K were found when and where chlorophyll concentrations exceeded 0.3 mg m^{-3}, but not specifically during the bloom peak. This suggests that nitrate inputs may have been the main reason for bloom generation and demise, but cannot explain the sudden chlorophyll increase in mid-April.

4.3. Iron Behavior From Lagrangian Floats

[14] In order to study a potential iron enrichment, we injected Lagrangian particles into the model along the western boundary, between 2°N and 2°S, below 80 m, in the core of the EUC defined as U > 80% MAX(U_{EUC}). The floats were launched every ten days, beginning with the

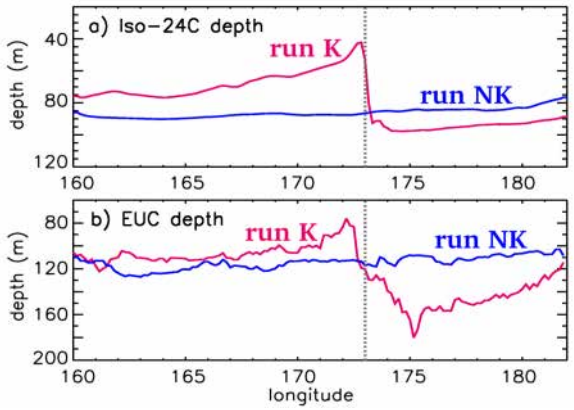

Figure 4. (a) 24°C-isotherm depth averaged between 0°N and 2°N and (b) EUC depth during the bloom generation (March–April 1998), in run K (red) and run NK (blue). Dots indicate the islands position.

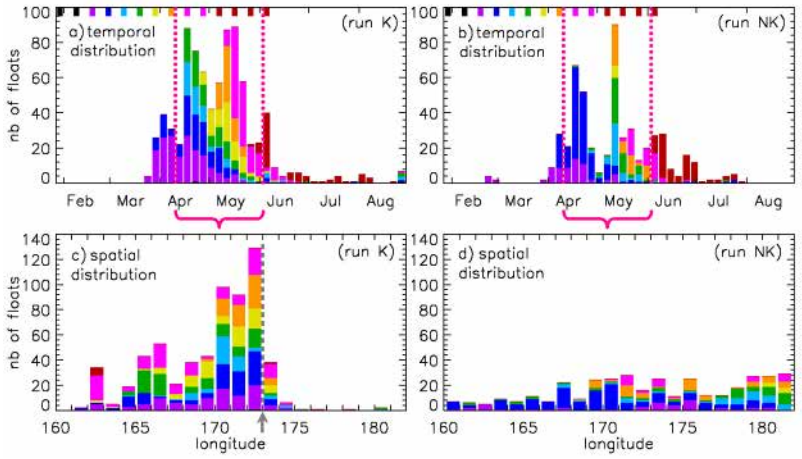

Figure 5. Number of floats originating from the EUC core entering the 50 m upper layer: temporal distribution ((a) run K, (b) run NK) and longitudinal distribution ((c) run K, (d) run NK) for the 10 April – 3 June 1998 period (vertical dotted lines in Figures 5a and 5b). Each color corresponds to the date of float introduction (indicated at the top of Figures 5a and 5b).

EUC recovery in late January. The timing and location of their arrival in the euphotic zone are shown in Figure 5, with each color representing a date of launch. Float arrival in run K (Figure 5a) was about one week late compared to the dramatic increase of chlorophyll concentration, which began around April 10. This may be because of a weakly modeled EUC. The floats setting during the bloom peak (Figure 5c) corresponded to that of the passive tracer and of the chlorophyll high concentrations. In run NK (Figures 5b and 5d), floats in the upper layer were much less numerous and more evenly distributed along longitudes.

[15] These numerical results indicate that local modification of the large-scale dynamics by the Kiribati Islands was able to enhance nutrient supply into the euphotic layer and to force it west of the archipelago. Iron input in the euphotic layer (suggested here by floats coming from the EUC core), which lagged behind nitrate supply (mimicked here by a passive tracer) by a few weeks was probably responsible for peaking of the chlorophyll bloom.

5. Conclusions

[16] Our results suggest that the small Kiribati Islands caused local perturbations of the large-scale equatorial dynamics specific to the El Niño/La Niña transition period, and as such were responsible for the strength and location of the bloom as follows.

[17] From January to April, an island mass effect induced a thermocline (nutricline) uplift and enhanced upwelling and vertical mixing west of the islands. The nitrate concentration increase was probably parallel to that of the simulated passive tracer, driving the bloom generation. Around mid-April, floats released in the EUC core reached the euphotic layer. They most likely represent a sudden input of iron due to the EUC shoaling enhanced by the islands obstacle, which explained the abrupt chlorophyll increase that led to the dramatic bloom observed in May. Finally, when the EUC outcropped and surface current reversed, oligotrophic waters were advected from the west, leading to the weakening and vanishing of the bloom in June.

[18] Similar blooms have not since been observed at this location, nor has the TAO time series at 165°E shown similar conditions. In the very specific context of the 1997–1998 El Niño/La Niña transition, the Kiribati Islands strongly affected chlorophyll concentrations near 170°E because they acted as an obstacle to both the SEC and the EUC. Compared to previous large-scale studies, careful examination of high-resolution data sets and model outputs revealed the significant impact of small islands on a comparatively huge biological event. However, a physical/biological model with nitrate and iron co-limitations, zooplankton, showing changes in phytoplankton species is needed to better understand the complex physical/biological interactions which occurred during this period.

[19] **Acknowledgment.** We would like to thank the TOGA-TAO Project Office run by M. J. McPhaden for sharing the time series data from the mooring array, Sophie Cravatte and Christophe Menkes for the OPA run we used, and Christophe Maes for his helpful comments.

References

Chavez, F. P., P. G. Strutton, G. E. Friederich, R. A. Feely, G. C. Feldman, D. G. Foley, and M. J. McPhaden (1999), Biological and chemical response of the equatorial Pacific Ocean to the 1997–98 El Niño, *Science*, *286*, 2126–2131.

Conkright, M. E., H. E. Garcia, T. D. O'Brien, R. A. Locarnini, T. P. Boyer, C. Stephens, and J. I. Antonov (2002), *World Ocean Atlas 2001* [CD-ROM], vol. 4, *Nutrients*, edited by S. Levitus, *NOAA Atlas NESDIS 52*, 392 pp., NOAA, Silver Spring, Md.

Gordon, R. M., K. H. Coale, and K. S. Johnson (1997), Iron distribution in the equatorial Pacific: Implications for new production, *Limmnol. Oceanogr.*, *43*, 419–431.

Heywood, K. J., D. P. Stevens, and G. R. Bigg (1996), Eddy formation behind the tropical island of Aldabra, *Deep Sea Res., Part I*, *43*, 555–578.

Murtugudde, R. G., S. R. Signorini, J. R. Christian, A. J. Busalacchi, C. R. McClain, and J. Picaut (1999), Ocean color variability of the tropical Indo-Pacific basin observed by SeaWiFS during 1997–1998, *J. Geophys. Res.*, *104*, 18,351–18,366.

Radenac, M.-H., C. Menkes, J. Vialard, C. Moulin, Y. Dandonneau, T. Delcroix, C. Dupouy, A. Stoens, and P.-Y. Deschamps (2001), Modeled and observed impacts of the 1997–98 El Niño on nitrate

and new production in the equatorial Pacific, *J. Geophys. Res.*, *106*, 26,879–26,898.

Ryan, J. P., P. S. Polito, P. G. Strutton, and F. P. Chavez (2002), Unusual large-scale phytoplankton blooms in the equatorial Pacific, *Progr. Oceanogr.*, *55*, 263–285.

Shchepetkin, A. F., and J. C. McWilliams (2005), The regional oceanic modeling system (ROMS): A split-explicit, free-surface, topography-following-coordinate oceanic model, *Ocean Modell.*, *9*, 347–404.

Stephens, C., J. I. Antonov, T. P. Boyer, M. E. Conkright, R. A. Locarnini, T. D. O'Brien, and H. E. Garcia (2002), *World Ocean Atlas 2001* [CD-ROM], vol. 1, *Temperature*, edited by S. Levitus, *NOAA Atlas NESDIS 49*, 167 pp., NOAA, Silver Spring, Md.

Wilson, C., and D. Adamec (2001), Correlations between surface chlorophyll and sea surface height in the tropical Pacific during the 1997–1999 El Niño–Southern Oscillation event, *J. Geophys. Res.*, *106*, 31,175–31,188.

J. Lefèvre, Centre IRD de Nouméa, BPA5, 98848 Nouméa cedex, New Caledonia.

P. Marchesiello, Centre IRD de Bretagne, BP 70, F-29280 Plouzané, France.

M. Messié and M.-H. Radenac, LEGOS, CNRS, IRD, UPS, CNES, 14 avenue Édouard Belin, F-31400 Toulouse, France. (monique.messie@legos.cnes.fr)